Micromechanics of Crack Growth into a Craze in a Polymer Glass

C. Y. Hui,*,†,‡ A. Ruina,†,‡ C. Creton,‡,§,⊥ and E. J. Kramer‡,§

Department of Theoretical and Applied Mechanics, the Material Science Center, and Department of Material Science and Engineering, Cornell University, Ithaca, New York 14853

Received February 14, 1992; Revised Manuscript Received April 24, 1992

ABSTRACT: The problem of craze failure near the tip of a crack embedded inside a craze is investigated in this work. Our micromechanics model is based on the presence of cross-tie fibrils in the craze microstructure. These cross-tie fibrils give the craze some small lateral load-bearing capacity so that they can transfer stress between the main fibrils. This load-transfer mechanism allows the normal stress on the fibrils directly ahead of the crack tip in the center of the craze to reach the breaking stress of the chains. An exact solution is obtained for the deformation field near the crack tip, and this solution is used to relate craze failure to the external loading and microstructural quantities such as the draw stress, the fibril spacing, and the chain breaking force. The relationship between energy flow to the crack tip due to external loading and the work of local fracture by fibril breakdown is also obtained. Our analysis shows that the normal stress σ_n acting on the fibrils at the crack tip increases linearly as the square root of the craze thickness assuming that the normal stress distribution is uniform and is equal to the drawing stress acting on the craze–bulk interface. However, our result shows that σ_n is very sensitive to the stress distribution at the craze–bulk interface so that the assumption of a constant draw stress acting on the craze–bulk interface ahead of the crack tip may underestimate σ_n. We also derived an approximate expression which relates the shear and tensile modulus of the crazed material to the underlying microstructural variables such as fibril spacing and fibril diameter.

1. Introduction

The fracture properties of most polymer glasses are linked to the stress-induced growth and breakdown of crazes, which are planar cracklike defects. However, unlike cracks, crazes are load bearing as their surfaces are bridged by many fine (5–30-nm-diameter) fibrils. As the crazes grow in width this fibril structure may break down, leading to large voids inside the craze which eventually grow to become cracks. The process of craze width growth and craze fibril breakdown are thus central to an understanding of the fracture mechanics of polymer glasses.

The best current micromechanics model for the growth of fibrils during craze widening is that of surface drawing; i.e., the craze grows in width by drawing new polymer material from a thin, strain softening layer at the craze–bulk interface ("the active zone") into the fibrils.[1] The width of this active zone is on the order of the fibril diameter and can be observed using a gold decoration technique.[2] Measurements of craze widening ahead of cracks have been made using transmission electron microscopy (TEM) and optical interference techniques.[3] From the amount of craze widening, the continuum stress acting in a direction normal to the craze–bulk interface can be deduced.[4] This normal stress or draw stress σ_d is found to be practically uniform along the entire length of the craze, with the exception of a very small region near the crack tip. In this region, there is a stress concentration which is difficult to quantify due to the limited resolution of optical microscopy and TEM.

The micromechanics of craze breakdown is not as well understood. One theory is that craze breakdown occurs by localized creep along the fibrils.[5] If this hypothesis were true, one would expect to see that voids nucleated most frequently in the midrib, the oldest portion of the craze which has a somewhat higher extension ratio than the rest due to it being drawn in the high stress zone just behind the craze tip. However, recent morphological observations[6,7] show that all the fibril breakdowns initiate at the craze–bulk interface. It should be noted that chain scission accompanying fibril surface formation at the bulk–craze interface alone is not sufficient to cause craze breakdown[8] so that fibril breakdown along the interface requires a loss of entanglement density. Indeed, a model of fibril failure based on chain scission and entanglement loss during the drawing process has led to satisfactory agreement with experimental results.[8] It should be noted that the craze breakdown results stated above correspond to the process of crack initiation in a defect-free craze. Such cracks, once initiated, grow by breaking down the fibril structure directly ahead of their tips. A mechanism of such craze breakdown has been proposed recently by Brown.[9] Previously the craze fibrils were modeled as straight parallel cylinders aligned along the normal to the craze surfaces and running from one craze interface to another. However, transmission electron micrographs and electron diffraction show the existence of short fibrils running between the main fibrils.[10,11] A model for the microstructure of the cross-tie fibrils is shown in Figure 1. These cross-tie fibrils give the craze some small lateral load-bearing capacity so that they can transfer stress between the main fibrils.[9] Brown[9] points out that this load-transfer mechanism allows the normal stresses on the fibrils directly ahead of the crack tip to reach the breaking stress of the chains. Brown develops a semiquantitative argument which gives the scaling of the stress concentration in the craze center with craze width and the anisotropic elastic properties of the crazed material. In this paper we build on Brown's approach and develop an analytical model with which we can rigorously examine the effect of various stress boundary conditions at the craze–bulk interface.

One of the difficulties in modeling the process of fibril breakdown near the tip of a crack inside the craze zone is the specification of the boundary conditions. The geometry of a crack inside a craze under external loading is illustrated schematically in Figure 2a. Figure 2b focuses on the area of interest Ω which is embedded in a region of length scale of order h, the length of the drawn fibrils

† Department of Theoretical and Applied Mechanics.
‡ The Material Science Center.
§ Department of Material Science and Engineering.
⊥ Present address: IBM Almaden Research Center, 650 Harry Rd., San Jose, CA 95120.

0024-9297/92/2225-3948$03.00/0

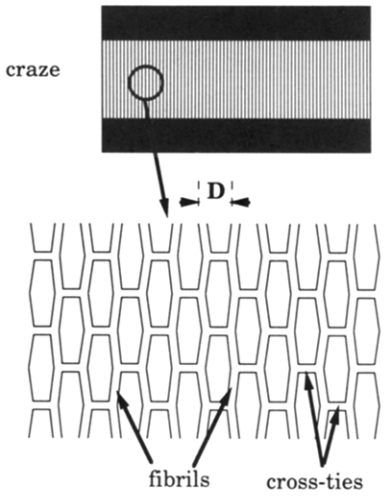

Figure 1. Schematic of craze microstructure.

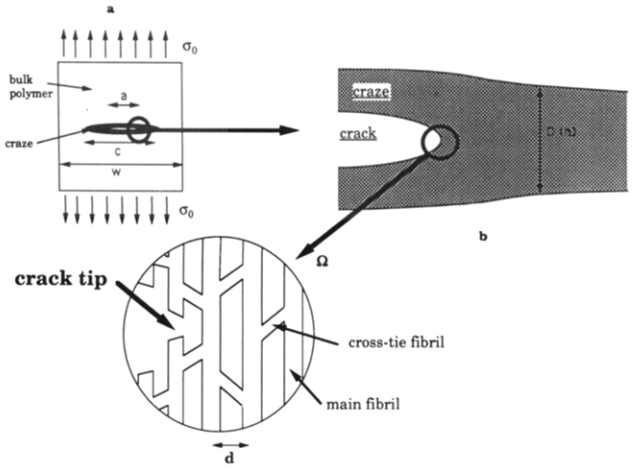

Figure 2. (a) Schematic diagram showing the geometry of a crack inside a craze under external loading. (b) Schematic diagram focusing on the area of interest Ω which is embedded in a region of length scale of order h, the length of the drawn fibrils inside the craze.

inside the craze. A typical length scale for Ω is d, the fibril spacing. Let a be the crack length and w the width of the specimen. Then, in general

$$w > c > a \gg h \gg d \tag{1a}$$

where c is the length of the craze + crack. The inequality $c > a \gg h$ allows us to model the crack and craze as infinite in extent with respect to h as shown in Figure 3. Since $h \gg d$, the bulk–craze interface is represented as a line (the external boundary of the strip) in Figure 3. Note that the condition $c > a \gg h$ is not the same as the "small scale yielding" (SSY) condition which requires the craze to be small compared with typical specimen dimensions, i.e.

$$a \gg c - a \quad \text{and} \quad w \gg c - a \tag{1b}$$

The main results of this paper do not depend on satisfying the SSY condition.

The material inside the strip consists of drawn main fibrils and cross-tie fibrils connecting them and was modeled as a linear anisotropic elastic material by Brown.[9] The difficulty lies on the specification of boundary conditions on the exterior boundary of the strip. It should be noted that the boundary traction depends on the fibril drawing process at the craze–bulk interface as well as the deformation response of the cross-tie fibrils inside the strip. An approximate but consistent way of specifying the boundary condition is to consider the strip as a line zone

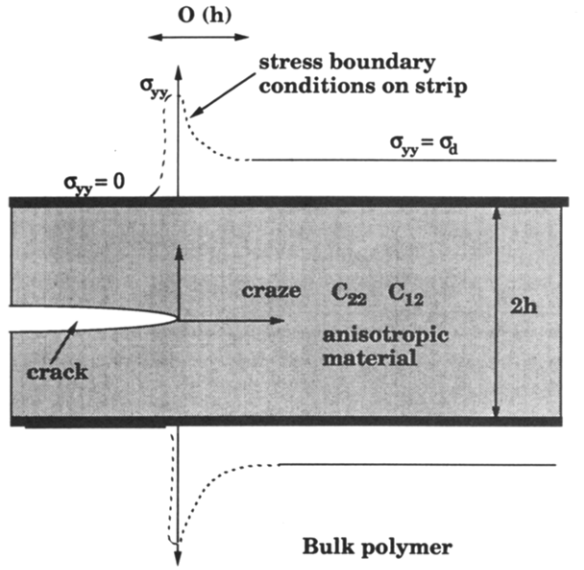

Figure 3. Geometry and boundary conditions of the micromechanics problem in which the craze material near the crack tip is modeled by an infinite strip of anisotropic linear elastic material with moduli C_{12} and C_{22}. The boundary of the strip represents the craze–bulk interface. The stress concentration on this boundary is indicated by the peak in σ_{yy}.

or a cohesive zone of zero thickness. This assumption is valid as long as the condition

$$c - a \gg h$$

is satisfied. Fortunately this condition is usually satisfied in experiments. Along the cohesive zone, normal displacement discontinuities are allowed in the continuum analysis. These displacement discontinuities are related to the traction history acting on the cohesive zone through the use of interface constitutive models. One such model which provides a good description of the shape and size of the craze zone at the crack tip is the well-known Dugdale model.[11,12] In this model, the normal stress along the craze zone is assumed to be constant and equal to σ_d. A limitation of the Dugdale model is that it cannot explain the stress concentration at the crack tip, as shown in Figure 3.

Brown[9] uses a displacement boundary condition so that the stress field near the crack tip subjected to this boundary condition could be found by consulting the appropriate literature. A more realistic boundary condition is to use the traction distribution of the Dugdale model; i.e., a uniform normal stress σ_d is prescribed on the part of the external boundary that lies ahead of the crack tip, i.e., $x = 0, y = h$ or $-h$. The traction on the rest of the external boundary as well as the crack faces is prescribed to be zero. As pointed out earlier, these boundary tractions may not be accurate in a small region near $0 < x < H = O(h)$ and $y = h$ or $-h$. In this work, the normal traction on $y = h$ or $-h$ will be prescribed so that it can take on any arbitrary form. The only restriction on the form of the normal traction is that it will approach the draw stress σ_d for $x > O(h)$. This approach will allow us to quantify the sensitivity of the fibril failure process to the crack tip stress concentration.

2. Model Description

The crack is assumed to be loaded under plane strain conditions so that the deformation field is independent of the out-of-plane coordinate. Under plane strain conditions there are only two nonvanishing components of the displacement field $u(x,y)$ and $v(x,y)$. The in-plane ge-

ometry and the loading are illustrated in Figure 3. The shear component of the traction vector, i.e., σ_{xy}, is prescribed to be zero on all external boundaries and on the crack faces. Also, $\sigma_{yy} = 0$ on the crack faces $x < 0$ and $y = 0$. The normal stress σ_{yy} on the external boundary $y = h$ or $-h$ is prescribed to be

$$\sigma_{yy} = \sigma_d f(x) \tag{2}$$

where $f(x)$ is a dimensionless function having the behavior

$$f(x) = 0 \quad \text{for } x < 0$$

$$f(x) \sim 1 \quad \text{for } x > H$$

where $H > 0$ and is on the order of h. As mentioned in the Introduction, a difficulty is to specify the boundary condition on the craze–bulk interface, i.e., $f(x)$. $f(x)$ can only be determined by coupling the process of fibril drawing to the stress analysis in both the crazed and uncrazed regions. This problem is highly nonlinear and is dependent on the model for drawing. In this paper, instead of analyzing the aforementioned problem, we consider various physically reasonable distributions $f(x)$ all having the property that σ_{yy} approaches the drawing stress at distances of order h ahead of the crack tip.

Following Brown,[9] the craze matter, consisting of main loading fibrils in the y direction connected sparsely by cross-tie fibrils, is modeled geometrically by an infinite strip of height $2h$. Its mechanical properties are modeled by assuming it to be a linearly elastic anisotropic material. In this work two more simplications, (1) $|u| \ll |v|$ in the strip and (2) ν, the Poisson ratio of the crazed matter, equals zero, are made. These conditions imply that $\sigma_{xx} = 0$ inside the strip and the nonvanishing strain components are ϵ_{yy} and ϵ_{xy}, respectively. These assumptions are reasonable for practically all material points in the craze with the exception of a small circular region of radius less than h centered at the crack tip, where the displacement u and σ_{xx} will not be zero. Because of symmetry, loading and the anisotropy in craze response to strain, even here σ_{xx} will be substantially less than σ_{yy}. On the basis of the above assumptions, the strain components are related to the stresses σ_{yy} and σ_{xy} by

$$\sigma_{yy} = C_{22}\epsilon_{yy} \quad \text{and} \quad \sigma_{xy} = 2C_{12}\epsilon_{xy} \tag{3}$$

where C_{22} and C_{12} are independent elastic moduli of the crazed material. In a later section, we will relate C_{22} and C_{12} to the underlying microstructure of the cross-tie fibrils. In the analysis that follows, C_{22} and C_{12} are assumed to be known positive material constants.

Consistent with the above simplications, the equilibrium equation of relevance is

$$\sigma_{yy,y} + \sigma_{xy,x} = 0 \tag{4}$$

where a subscript comma denotes the partial derivative with respect to the subscript. Substituting $\epsilon_{yy} = v_{,y}$ and $2\epsilon_{xy} = v_{,x}$ into eqs 3 and 4, we obtain

$$C_{22}v_{,yy} + C_{12}v_{,xx} = 0 \tag{5}$$

This is the partial differential equation governing the deformation field inside the infinitely long racked strip with height $2h$.

The following dimensionless variables are introduced to expedite the analysis:

$$X = x/(h\alpha)$$

$$Y = y/h \tag{6}$$

$$V = v/h$$

where α^2 is a dimensionless material constant defined by

$$\alpha^2 = C_{12}/C_{22} \tag{7}$$

Using eqs 6 and 7, eq 5 becomes

$$V_{,XX} + V_{,YY} = 0 \tag{8}$$

i.e., the Laplace equation. Thus, assumptions 1 and 2 allow us to consider a much simpler mathematical problem. The boundary conditions appropriate for the solution of eq 8 are

$$\sigma_{yy} = \sigma_d F(X) = \sigma_d f(h\alpha X) \qquad Y = 1 \text{ or } -1 \tag{9}$$

and the traction-free boundary condition on the crack faces reduces to

$$\sigma_{yy} = 0 \qquad Y = 0 \qquad X < 0 \tag{10}$$

In particular, if we *define*

$$\Sigma_2 = \sigma_{yy}/C_{22} \quad \text{and} \quad \Sigma_1 = \sigma_{xy}/C_{22}\alpha \tag{11}$$

then the constitutive model eq 3 becomes

$$\Sigma_1 = V_{,X} \quad \text{and} \quad \Sigma_2 = V_{,Y} \tag{12}$$

respectively. The equilibrium eq 4 becomes, under these transformations

$$\Sigma_{1,X} + \Sigma_{2,Y} = 0 \tag{13}$$

Equations 8, 12, and 13 can be interpreted as an antiplane shear problem in the (X, Y) plane if we identify V as the antiplane shear displacement and Σ_1 and Σ_2 as the normalized shear stresses, respectively. A concise description of the antiplane shear problem can be found in Rice.[14] In terms of the new variables Σ_1 and Σ_2, the boundary conditions in eqs 9 and 10 can be rewritten as

$$\Sigma_2 = \sigma_d F(X)/C_{22} = \sigma_d f(h\alpha X)/C_{22} \qquad Y = 1 \text{ or } -1 \tag{14}$$

$$\Sigma_2 = 0 \qquad Y = 0 \text{ and } X < 0 \tag{15}$$

The exact solution of this problem is presented in the next section.

3. Results and Discussion

The stress fields everywhere inside the strip can be represented by an analytic function $\phi(z) = \Sigma_2 + i\Sigma_1$ where $z = X + iY$ and i is the complex number defined by $i = (-1)^{1/2}$. Σ_2 and Σ_1 are related to the actual stresses σ_{yy} and σ_{xy} via eq 11. Using the detailed process of solution given in the appendix, $\phi(z)$ is found to be

$$\Sigma_2 + i\Sigma_1 = \int_{-\infty}^{-1} e^{\pi z}(e^{\pi z} - 1)^{-1/2}(1 - t)^{1/2}(t - e^{\pi z})^{-1} g(t)\, dt \tag{16}$$

where $g(t) = (\sigma_d/\pi t C_{22}) f(h\alpha \ln |t|/\pi)$. Equations 16 and 11 imply that the stresses have a square-root singularity at the crack tip. In particular, directly ahead of the crack tip, i.e., $y = 0$, the asymptotic behavior of the stress σ_{22} can be found using eqs A8, 3, and 6:

$$\sigma_{22} = K_{tip}(2\pi x)^{-1/2} \tag{17}$$

where K_{tip} is given by

$$K_{tip} = \sigma_d(2h/\alpha)^{1/2} \int_0^\infty f(ht)\, [1 + \exp(\lambda t)]^{-1/2}\, dt \tag{18}$$

where $\lambda = \pi\alpha^{-1}$. The subscript "tip" in K_{tip} is used to

distinguish K_{tip} from the applied stress intensity factor K_A. K_A is the amplitude of the stress field near the tip of a crack of length a embedded in a linearly elastic material which models the material behavior of the polymer glass outside the craze. K_A uniquely characterizes the loading sensed by the crazed region ahead of the crack if the SSY condition in eq 1a is satisfied.

Note that $\lambda \gg 1$ since α is generally small. The condition $\lambda \gg 1$ and the rapid decay of the exponential factor in eq 18 as one moves away from $t = 0$ means that, for the case of small α, the contribution of the integrand tends to be confined, in a more and more concentrated fashion, to the neighborhood of $t = 0$ as λ increases. In other words, for small α, K_{tip} depends mainly on the behavior of the traction on the part of the cohesive zone nearest to the crack tip. We shall demonstrate this dependence below.

The dependence of K_{tip} on the traction distribution $f(x)$ can be studied using eq 18. The simplest case is to assume

$$f(x) = 1 \quad x > 0$$

$$f(x) = 0 \quad x < 0 \tag{19}$$

The stress intensity factor K_{tip} can be evaluated exactly in this case, and it is

$$K_{tip} = A\sigma_d[\alpha h]^{1/2} \tag{20}$$

where $A = 2^{1/2}\pi^{-1} \ln \{(2^{1/2}+1)(2^{1/2}-1)^{-1}\} \sim 0.794$. Note that K_{tip} is proportional to σ_d and $\alpha^{1/2} = (C_{12}/C_{22})^{1/4}$ so that $K_{tip} = 0$ if $C_{12} = 0$. Thus, there is no stress concentration at the crack tip without the cross-tie fibrils, in agreement with the results of Brown.[9] Furthermore, K_{tip} is proportional to $h^{1/2}$ so that the stress concentration increases linearly as the square root of the craze width. This result is also in agreement with Brown's.[9]

Consider now the case where stress concentrations exist on the external boundaries $y = h$ and $-h$. As pointed out in section 1 and illustrated by Figure 1, a region of high normal stress occurs near $x = 0, y = h$ or $-h$. Specifically, we assume the normal stress distribution has the form

$$f(x) = 0 \quad x < 0$$

$$f(x) = 1 \quad x > H$$

$f(x)$ is assumed to have a maximum f^* where $f^* > 0$ at $x = 0$, and f can have arbitrary behavior in $[0, H]$ provided that it is independent of α. For $\alpha \ll 1$, K_{tip} is approximately given by

$$K_{tip} = A_c\sigma_d[\alpha h]^{1/2} \tag{21}$$

where $A_c = Af^*$. Note that $A_c \gg A$ if $f^* \gg 1$ so that K_{tip} in eq 21 is much larger than K_{tip} given by eq 20. Also, as long as the condition $\alpha \ll 1$ is satisfied, K_{tip} is approximately independent of the spatial distribution of f in the region $x > 0$. The validity of eq 21 is justified in Appendix 3.

It is also possible to include singular stress distributions as boundary conditions. If f has singularities of the form $f(x) = f^*(x/h)^{-\beta}$ as x approaches zero, $x > 0$, then for $\alpha \ll 1$

$$K_{tip} = A_c\sigma_d h^{1/2}\alpha^b \quad \text{for } \beta < 1 \tag{22}$$

where $b = 0.5 - \beta$ and $A_c = [\pi/2]^{(-1+\beta)}2^{1/2}f^*I(-\beta)$. $I(-\beta)$ is defined by the integral

$$I(-\beta) = \int_0^\infty u^{-\beta}e^{-u}[1 + e^{-2u}]^{-1/2}\,du$$

Since $2^{-1/2} < [1 + e^{-2u}]^{-1/2} < 1$ for all $u > 0$, $2^{-1/2} < I(-\beta)/\Gamma(1-\beta) < 1$. Note that A_c is of order 1, but the dependence of K_{tip} on $\alpha = (C_{12}/C_{22})^{1/2}$ has changed. Indeed, for $^1/_2 < \beta < 1$, $b < 0$ and K_{tip} becomes unbounded as α approaches zero. Physically, this means that fibrils without cross-ties are unstable at the crack tip irrespective of their length. Furthermore, singularities of the form $f(x) = f^*(x/h)^{-\beta}$ for $^1/_2 < \beta < 1$ give rise to infinite elastic strain energy in a linearly elastic material. Therefore, it is highly unlikely that the normal stress distribution at the craze–bulk interface is given by $f(x) = f^*(x/h)^{-\beta}$ with $^1/_2 < \beta < 1$. Note that eq 21 is a special case of eq 22; i.e., it can be obtained by setting $\beta = 0$.

A particular case of $f(x)$ having a singularity of the form $f(x) = f^*[-\ln (x/h)]^\beta$, where $0 < \beta < 1$, as x approaches zero, is worth considering. In this case, K_{tip} is approximately given by

$$K_{tip} = Af^*\sigma_d h^{1/2}\alpha^{1/2}(-\ln \alpha)^\beta \tag{23}$$

for $\alpha \ll 1$. This case is important because the near-tip normal stress directly ahead of a steadily quasi-statically growing crack with velocity $\dot{s}$ along the positive x direction has the asymptotic form

$$\sigma_{yy} = f^*\sigma_d[-\ln (x/h)]^\beta \tag{24}$$

where f^* is defined by

$$f^* = c[4\pi\sigma_d\dot{s}(1 - \nu_g^2)/(\omega E)]^\beta$$

$$\beta = 1/(n-1)$$

$$c = [(n-1)/(n\pi^2)]^{-\beta} \tag{25}$$

This near-tip field was derived under the assumption that the crazed material directly ahead of the propagating crack draws according to

$$\begin{aligned} D\delta/Dt &= \omega[\sigma_{yy}/\sigma_d - 1]^n \quad \sigma_{yy} > \sigma_d \\ &= 0 \quad \sigma_{yy} < \sigma_d \end{aligned} \tag{26}$$

where n is in general much larger than 1 and ω is a material parameter.[15] δ is the excess normal displacement between two material points on opposing sides of the interface over that which would be predicted by the laws of bulk deformation of the material. $D\delta/Dt$ is the material time derivative of δ. When $n \gg 1$, $D\delta/Dt = B[\sigma_{yy}]^n$ approximately describes the response of the interface due to the drawing of fibrils into the craze. Note that the stress is weakly dependent on the crack velocity and the resistance to drawing as characterized by the parameter ω. In general, an increase in crack growth rate or a decrease in ω will increase the stress near the crack tip region and hence increases K_{tip}. Equations 21–23 show that K_{tip} is significantly affected by the details of stress concentration on the craze–bulk interface. In general, the higher this stress concentration, the higher is K_{tip}.

Finally, a closed form solution for the full field in Ω can be obtained for the case of

$$f(x) = 1 \quad x > 0$$

$$f(x) = 0 \quad x < 0$$

Details are given in Appendix 1. The solution is

$$\Sigma_2 + i\Sigma_1 = (\sigma_d/C_{22})\{b(e^{\pi z} - 1)^{-1/2} + 1 - 2\pi^{-1}\tan^{-1}[2/(e^{\pi z} - 1)]^{1/2}\}$$

$$b = \pi^{-1}\ln\{(2^{1/2}+1)(2^{1/2}-1)^{-1}\} \tag{27}$$

where $2\tan^{-1} u = i\,\mathrm{Ln}\,[(u+i)/(-u+i)]$ and Ln is the principal branch of the logarithm function, with the branch cut being the negative u axis. Directly ahead of the crack tip, $\sigma_{yy} = \sigma_d b\{(e^{\pi x/\alpha h}-1)^{-1/2} + 1 - 2\tan^{-1}[2/(e^{\pi x/\alpha h}-1)]^{1/2}\}$ so that the tensile stress σ_{yy} decreases exponentially fast with characteristic distance αh to the crazing stress σ_d. Note that, because of the factor α in eq 11, the magnitude of the shear stress is much less than that of σ_{yy}.

Energy Considerations. Since the material outside the craze region is modeled as elastic, the only source of mechanical energy dissipation is the craze zone near the crack tip. Energy is dissipated via the process of drawing in the bulk–craze interface and the process of fracture through fibril breakdown at the crack tip.

Consider an isolated crack in a specimen. Assume the crack and the craze is growing at a constant rate $\dot{s}_{SS}$ and a contour γ is fixed with respect to the moving craze tip. This contour γ can be any piecewise smooth curve which surrounds the crack tip and the craze zone, starting from the lower traction-free crack face and ending on the upper traction-free crack face. It is to be transversed in the counterclockwise sense; its arc length will be denoted by s. Define the integral J by

$$J = \int_\gamma \sigma_{ij}\epsilon_{ij}/2\,\mathrm{d}y - \sigma_{ij}n_j u_{i,x}\,\mathrm{d}s$$

where subscript, x denotes the partial derivative with respect to x and n_j are the components of the normal vector to the curve γ. It can be shown that J is independent of γ. Furthermore, $J\dot{s}_{SS}$ is equal to the time rate of energy flow to the crazed zone.[16] Furthermore, under the SSY condition in eq 1b, $J = \mathcal{G}$, where $\mathcal{G}$ is the energy release rate and is equal to

$$(1-\nu_g^2)K_A^2E^{-1} \tag{28}$$

where K_A is the stress intensity factor for the specimen with a sharp structureless crack tip. E and ν_g are Young's modulus and Poisson's ratio of the polymer glass outside the craze. K_A will be referred to as the applied stress intensity factor. Let E_d be the energy dissipated by the fibril drawing process on the craze–bulk boundary per unit crack extension. According to the Dugdale model

$$E_d = \sigma_d\delta_{tip} \tag{29}$$

where δ_{tip} is related to the measured zone thickness $2h$ at the crack tip by

$$\delta_{tip} = 2h(1-\nu_f) \tag{30}$$

where ν_f is the ratio of the density of the crazed material to the density of the material in the surrounding homogenous polymer.[17] Experiments on crazes in glassy polymers have shown that ν_f is practically uniform throughout the entire craze zone (i.e., $\nu_f = 0.25$ in polystyrene) with the exception of a small region near the crack and craze tip.[1] In this region, ν_f decreases from its average value of 0.25–0.2. It should be noted that the assumption $c - a \gg h$ is consistent with most experimental results. Then energy conservation and the lack of other deformation processes imply that

$$E_f = J - E_d \tag{31}$$

where E_f is the energy available for fracture per unit crack extension.

E_f can be estimated using our strip model. From linear elastic fracture mechanics[12]

$$E_f = (K_{tip})^2/2C_{22} \tag{32}$$

It is interesting to compare the magnitudes of E_f and E_d. Using eqs 29–30 and 32, the ratio of E_f/E_d is found to be

$$E_f/E_d = A_c^2(\sigma_d/C_{22})\alpha[4(1-\nu_f)]^{-1} \tag{33}$$

Since C_{22} is on the order of E which is about 3 GPa for most polymer glass and σ_d is about 30 MPa for PS, σ_d/C_{22} is on the order of 10^{-2}. Furthermore, $\alpha \ll 1$ and $A_c = 0.637$ so that $E_f/E_d = 0$ for all practical purposes. This result points out that most of the energy flow to the crack tip region is dissipated through plastic deformation and that only a very small amount of energy is needed for the actual fracture process. This observation implies that

$$J \sim E_d \sim \sigma_d\delta_{tip} \tag{34}$$

Finally, it should be noted that, in general, J does not equal $(1-\nu_g^2)K_A^2/E$ except under SSY conditions.[14]

Relation of K_{tip} to External Loads. The most general relation between K_{tip} and external loading can be obtained using eqs 21 and 34; i.e.

$$K_{tip} = A_c[\sigma_d\alpha J/2(1-\nu_f)]^{1/2} \tag{35}$$

Equation 35 does not depend on the SSY condition. However, J in this case depends on the specimen geometry, the elastic constants of the polymer outside the craze zone, and the interface model as indicated by eq 35. The usage of more realistic interface models and specimen geometry will undoubtedly complicate the evaluation of J. Under SSY conditions, J is given by eq 28; then eq 35 becomes

$$K_{tip} = A_cK_A[\sigma_dE^{-1}\alpha(1-\nu_g^2)/2(1-\nu_f)]^{1/2} \tag{36}$$

The factor $[\sigma_dE^{-1}\alpha]^{1/2}$ in eq 36 implies that $K_{tip} \ll K_A$. Equation 36 is much easier to use than eq 35 as K_A for different specimens and loading conditions can be obtained from handbooks.[18]

Fracture Criterion. The analysis above shows that the stress field at the crack tip has a square-root singularity as long as $K_{tip} > 0$. Clearly the results of the continuum analysis cannot be applicable at the crack tip. However, one could set as a fracture criterion

$$\sigma_{22}(x=d,y=0) = \sigma_f = \Sigma'\mathbf{f}_b \tag{37}$$

where Σ' is the effective number of polymer chains per unit surface area and $\mathbf{f}_b$ is the force required to break a polymer backbone. The parameter d is on the order of the fibril diameter and is assumed to be much less than h so that

$$\sigma_{22} \sim K_{tip}(2\pi x)^{-1/2} \tag{38}$$

in the neighborhood of $x = d$. Fracture occurs when

$$K_{tip} = \Sigma'\mathbf{f}_b(2\pi d)^{1/2} \tag{39}$$

Using eqs 36 and 39, the critical applied stress intensity factor K_{IC} for crack advance under SSY conditions is

$$K_{IC} = [A^*(\sigma_d/E)(C_{12}/C_{22})^{1/2}/2\pi d]^{-1/2}\Sigma'\mathbf{f}_b \tag{40}$$

where $A^* = A_c^2(1-\nu_g^2)/2(1-\nu_f)$. Equation 40 can also be expressed in terms of the bulk fracture toughness $\mathcal{G}_{IC}$; i.e.

$$\mathcal{G}_{IC} = A_c^{-2}(1-\nu_f)4\pi d(C_{22}/C_{12})^{1/2}(\Sigma'\mathbf{f}_b)^2/\sigma_d \tag{41}$$

where $A_c^2 = (0.794f^*)^2$. For the case of no stress concentration, i.e., $f^* = 1.0$, our expression for $\mathcal{G}_{IC}$ differs from Brown's[9] by a factor of approximately 1.

Discussion. Two simple micromechanic models of the craze structure are used to estimate C_{12}. Both models are two-dimensional models which neglect the deformation of the vertical main fibrils. In the first model shown in Figure 4, the cross-tie fibrils are treated as cylindrical

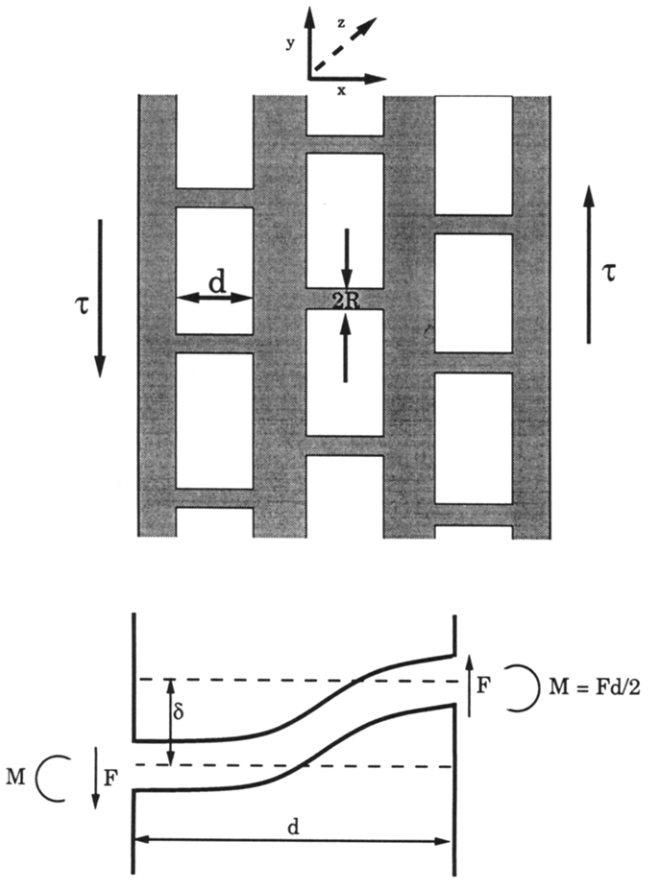

Figure 4. Geometry of the craze fibrils for the beam model. This model is used to estimate the shear modulus C_{12}. The figure on the bottom shows the force acting at the ends of a typical cross-tie fibril.

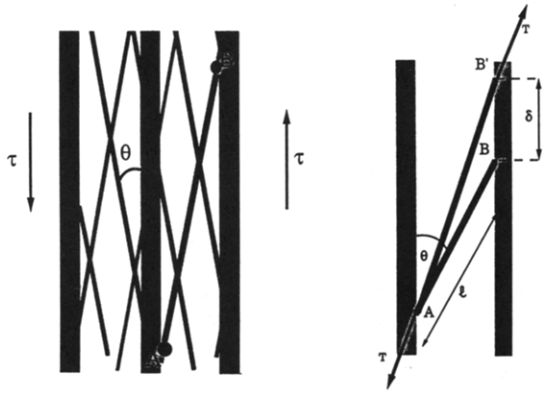

Figure 5. Geometry of the craze fibrils for the stretching model. This model is used to estimate the shear modulus C_{12}. The figure on the right-hand side shows the loading and deformation of the fibril AB.

elastic beams with length d and radius R. In the second model shown in Figure 5, the bending effects are neglected and the deformation of each cross-tie fibril is limited to stretching only. As shown in Appendix 2, these two models give an upper estimate for C_{12}. The resulting C_{12}/C_{22} for the beam model is

$$C_{12}/C_{22} = (3\pi f_c/8f_m)(R/d)^2 \tag{42}$$

where f_c and f_m are the volume fractions of the cross-tie fibrils and the main fibrils, respectively. d_c is the length of the cross-tie fibrils and is nearly equal to the average spacing between the main fibrils. The resulting C_{12}/C_{22} for the stretching model is

$$C_{12}/C_{22} = (f_c\theta^2/f_t) \tag{43}$$

where θ is the inclination of the cross-tie fibrils with respect to the vertical main fibrils, as shown schematically in Figure 5. In eq 43, f_t is the total volume fraction of the fibrils. Equation 43 is derived under the assumption that $\theta \ll 1$ so that $\sin\theta \sim \theta$. For $d_c/R = 4 = f_m/f_c$, C_{12}/C_{22} is found to be 0.018 for the beam model. For $\theta = 10°$, C_{12}/C_{22} is found to be 3.1×10^{-2} for the stretching model.

These results for C_{12}/C_{22} can be used to obtain an estimate of the force to break a single chain from eq 41 if the other parameters are known. In the measurement of interfaces between polystyrene (PS) and poly(2-vinylpyridine) (PVP) reinforced with PS–PVP block copolymer recently investigated by Creton et al.,[19] typical values are $\mathcal{G}_{IC} = 100$ J/m^2, $d = 10$ nm, σ_d(PS) = 55 MPa, $\Sigma' = 0.1$ chains/nm^2, and $A_c = 0.794$, i.e., $f^* = 1$; we have $\mathbf{f}_b = 9.9 \times 10^{-10}$ N for the first model and $\mathbf{f}_b = 1.1 \times 10^{-9}$ N for the second model which are both reasonable values.

Finally, in the evaluation of K_{tip}, we have assumed that $f(x) = 0$ for $x < 0$ so that there is no traction on the craze face behind the crack tip. Physically, the crack tip is located where the last fibril break occurs. Note that, because of the cross-tie fibrils, the craze material immediately behind the last broken fibril is still load bearing. The location of the crack tip in the continuum analysis should correspond to where the craze material behind the crack tip ceases to be load bearing, say, $x < -H_1$, and not the physical crack tip. Indeed, if $f(x)$ is assumed to behave as

$$f(x) = 0 \qquad x < -H_1$$

$$f(x) > 0 \qquad -H_1 < x$$

then K_{tip} is given by

$$K_{tip} = \sigma_d(2h/\alpha)^{1/2}\int_{-H_1/h}^{\infty} f(ht)\,[1 + \exp(\lambda t)]^{-1/2}\,dt \tag{44}$$

instead of eq 18. Note that, for small α, it is no longer true that K_{tip} is proportional to $\alpha^{1/2}$. Indeed, if $f(x) = 1$ for $-H_1 < x$, K_{tip} can be evaluated exactly and is found to be

$$K_{tip} = [2\alpha h]^{1/2}\sigma_d \ln\{(\beta^{1/2} + 1)/(\beta^{1/2} - 1)\} \tag{45}$$

where $\beta = 1 + \exp(-\lambda H_1/h)$. For sufficiently small $\alpha,\beta \sim 1$ and eq 45 becomes

$$K_{tip} = [2\alpha h]^{1/2}\sigma_d(\ln 4 + \lambda H_1/h)/\pi \sim [\alpha h/2]^{-1/2}\sigma_d H_1$$

so that K_{tip} is proportional to $\alpha^{-1/2}$! In general, one can verify that, for sufficiently small α, K_{tip} is given approximately by

$$K_{tip} = \sigma_d(2h/\alpha)^{1/2}\{\int_{-H_1/h}^{0} f(ht)\,dt + O(\alpha)\} \tag{46}$$

if $f(x)$ is bounded at $x = 0$. Thus, our earlier results in eqs 21 and 22 are valid only if f vanishes sufficiently fast in $-H_1 < x$ so that $\int_{-H_1/h}^{0} f(ht)\,dt \ll \alpha$.

Acknowledgment. Support by the Material Science Center at Cornell University, which is funded by the National Science Foundation (DMR-MRL program), is gratefully acknowledged by C.C., E.J.K., and C.Y.H. We greatly appreciate H. R. Brown for informative discussions.

Appendix 1

Symmetry consideration allows us to solve the Laplace equation (8) inside the infinite strip $\Omega = \{(X,Y), 0 < Y < 1\}$ subjected to the boundary conditions

$$\Sigma_1(X > 0, Y = 0) = 0$$

$$\Sigma_2(X < 0, Y = 0) = 0$$

$$\Sigma_2(X, Y = 1) = \sigma_d F(X)/C_{22} = \sigma_d f(h\alpha X)/C_{22} \quad \text{(A1)}$$

Let $z = X + iY = (x\alpha^{-1} + iy)/h$ be a point in the physical plane Ω and $s = p + iq$ be a point in the transformed plane, where $i = (-1)^{1/2}$. It is easy to show that the mapping

$$s = \Psi(z) = e^{\pi z} \quad \text{(A2)}$$

maps Ω into the upper half of the s plane conformally. Under the mapping Ψ, lines that are horizontal in Ω are mapped to rays emanating from the origin in the upper half of the s plane and lines that are vertical in Ω are mapped to semicircles with a common center at the origin in the s plane. In particular, the boundary $Y = 1$ is mapped onto the negative p axis; the upper crack face $X < 0$, $Y = 0^+$ is mapped onto the unit interval (0, 1) on the p axis. The crack tip $z = 0$ is mapped to the point $s = 1$. The inverse mapping $z = \Psi^{-1}(s)$ is given by $\pi^{-1} \ln s$ where

$$\ln s = \ln |s| + i \arg s \qquad 0 < \arg s < \pi \quad \text{(A3)}$$

Since the Laplace equation is preserved under conformational mapping, one can define a corresponding set of stresses $\Phi_2 + i\Phi_1$ in the s plane. $\Sigma_2 + i\Sigma_1$ in the physical plane is related to $\Phi_2 + i\Phi_1$ in the s plane by

$$\Phi_2 + i\Phi_1 = (\Sigma_2 + i\Sigma_1)e^{-\pi z}\pi^{-1} \quad \text{(A4)}$$

The corresponding boundary conditions for the transformed upper half of the s plane are

$$\Phi_1 = 0 \qquad s > 1$$

$$\Phi_2 = 0 \qquad 0 < s < 1$$

$$\Phi_2 = (\sigma_d/\pi p C_{22}) f(h\alpha \ln |p|/\pi) \qquad s < 0 \quad \text{(A5)}$$

Physically, the boundary value problem specified by eq A5 corresponds to a semiinfinite crack loaded under antiplane shear conditions. The crack occupies the interval $p < 1$ and $q = 0$ with the crack tip at $s = 1$. It is loaded by the traction

$$\Phi_2 = 0 \qquad 0 < s < 1$$

$$\Phi_2 = (\sigma_d/\pi p C_{22}) f(h\alpha \ln |p|/\pi) \qquad s < 0 \quad \text{(A6)}$$

on the crack faces. The solution of this problem is well-known and is given by

$$\Phi_2 + i\Phi_1 = \pi^{-1}(s-1)^{-1/2}\int_{-\infty}^{0}(1-t)^{1/2}(t-s)^{-1}g(t)\,dt \quad \text{(A7)}$$

where $g(t) = (\sigma_d/\pi t C_{22}) f(h\alpha \ln |t|/\pi)$ and we have used the traction-free boundary condition on the crack faces. An explicit form of $\Sigma_2 + i\Sigma_1$ can be found in terms of X and Y using eqs A2, A3, and A7; i.e.

$$\Sigma_2 + i\Sigma_1 = e^{\pi z}(e^{\pi z} - 1)^{-1/2}\int_{-\infty}^{-1}(1-t)^{1/2}(t - e^{\pi z})^{-1}g(t)\,dt \quad \text{(A8)}$$

where we have used the condition that $f = 0$ for all $x < 0$ so that the integration limit ends at $t = -1$ instead of $t = 0$.

The asymptotic behavior of $\Sigma_2 + i\Sigma_1$ as z approaches zero can be obtained from eq A8; i.e.

$$\Sigma_2 + i\Sigma_1 \sim Bz^{-1/2}$$

where $B = -\pi^{-1/2}\int_{-\infty}^{-1}(1-t)^{-1/2}g(t)\,dt$.

In particular, directly ahead of the crack tip, i.e., $y = 0$, the asymptotic behavior of the stress σ_{22} can be found using eqs A8, 6, and 11:

$$\sigma_{22} = K_{tip}(2\pi x)^{-1/2}$$

where K_{tip} is given by

$$K_{tip} = \sigma_d(2h/\alpha)^{1/2}\int_0^\infty f(ht)\,[1 + e^{\lambda t}]^{-1/2}\,dt \quad \text{(A9)}$$

where $\lambda = \pi\alpha^{-1}$.

For the special case of $f(x) = 1$ for all $x > 0$ and 0 otherwise, an exact solution can be obtained by directly integrating eq A8; i.e.

$$\Sigma_2 + i\Sigma_1 = (\sigma_d/C_{22})\{b(e^{\pi z} - 1)^{-1/2} + 1 - 2\pi^{-1}\tan^{-1}[2/(e^{\pi z} - 1)]^{1/2}\}$$

$$b = \pi^{-1}\ln\{(2^{1/2} + 1)(2^{1/2} - 1)^{-1}\} \quad \text{(A10)}$$

where $2\tan^{-1} u = i\,\mathrm{Ln}\,[(u + i)/(-u + i)]$ and Ln is the principal branch of the logarithm function, with the branch cut being the negative u axis. Note that, directly ahead of the crack tip

$$\Sigma_2 = (\sigma_d/C_{22})\{b(e^{\pi x/\alpha h} - 1)^{-1/2} + 1 - 2\pi^{-1}\tan^{-1}[2/(e^{\pi x/\alpha h} - 1)]^{1/2}\}$$

so that the tensile stress σ_{22} decreases exponentially fast with a characteristic distancee αh to the norminal value of σ_d.

Appendix 2

The top part of Figure 4 shows the geometry of the craze fibrils for the beam model. We assume that all the cross-tie fibrils are lined up with the x direction and that all the main fibrils are lined up with the y direction. The cross-tie fibrils are treated as cylindrical elastic beams with length d and radius R. d is equal to the average edge to edge spacing between the main fibrils. In the beam model, deformation of the main fibrils is neglected. The only deformation for which we account is bending of the cross-tie fibrils. A continuum element which includes many fibrils under a uniform shear τ is illustrated in Figure 4. Let n be the number of cross-tie fibrils per unit area in the yz plane, and let F be the force acting at the ends of a typical cross-tie fibril inside this continuum element as shown in the bottom part of Figure 4. The average shear stress τ on the continuum element is given by $\tau = nF$. The displacement δ of one end of the beam relative to the other end is related to the average shear strain γ of the element via the relationship $\delta = \gamma d$. Simple beam theory gives $\delta = Fd^3/3E\pi R^4$ so that

$$\gamma = \tau d^2/3En\pi R^4 \quad \text{(A11)}$$

where we have assumed that Young's moduli E of the main fibrils and the cross-tie fibrils are the same. Since $C_{12} = \tau/\gamma$, we have, from eq 11

$$C_{12}/E = 3f_c R^2/d^2 \quad \text{(A12)}$$

where we have used the volume fraction of cross-tie fibrils $f_c = n\pi R^2$. Equation 40 is obtained by noting that $E =$

C_{22}/f_m. The estimate given by eq 40 is an upper estimate since the deformation of the main fibrils is neglected.

In the second model, the cross-tie fibrils are obtained by overlaying the main tensile fibril grid with a second grid of fibrils which are rotated slightly from the main tensile fibrils. Such a secondary grid (with fibrils oriented at $\pm\theta$ to the primary grid) is shown on the left-hand side of Figure 5. We shall assume that the main fibrils do not deform in shear and that shear stiffness arises from the stretch of the secondary grid. Let A and B be the two ends of a typical cross-tie fibril as illustrated in Figure 5. We shall assumed that A and B only move up and down along the main fibrils so that there is no transverse extension strain. We apply a shear stress τ_{xy} on the surface with normal in the $+x$ direction of the continuum element on the left-hand side of Figure 5, where n is the number of cross-tie fibrils per unit area. Then the tensile strain ϵ along a typical cross-tie fibril (e.g., AB) is given by $\epsilon = \delta \cos\theta/l$ where l is the length of AB and δ is the relative vertical displacement of the ends A and B as shown on the right-hand side of Figure 5. The tension force T along AB is given by $EA\epsilon$, where A is the cross-sectional area of the cross-tie fibril. The shear stress can be related to the cross-tie tension by $\tau_{xy} = n\mathbf{T}\cos\theta$. The shear strain γ is related to the main fibril spacing d by $\delta/d = \gamma$. Eliminating δ we have $\tau = \gamma ndEA\cos^2\theta/l$ so that

$$C_{12} = \tau/\gamma = ndEA\cos^2\theta/l \tag{A13}$$

Using the fact that the volume fraction of cross-tie fibrils f_c is related to n by $nA/\sin\theta$ and $d/l = \sin\theta$, eq A13 becomes

$$C_{12} = Ef_c(\sin 2\theta)^2/4 \tag{A14}$$

If we use the small-angle approximations that $\cos\theta = 1$ and $\sin\theta = \theta$, then C_{22} is related to E by $C_{22} = Ef_t$ where f_t is the total volume fraction of the fibrils. Equation A14 becomes

$$C_{12}/C_{22} = f_c\theta^2/f_t$$

Appendix 3

To obtain eq 22, we need to find the asymptotic behavior of integrals of the form

$$\varphi(\lambda) = \int_0^\infty f(t)\,[1 + e^{\lambda t}]^{-1/2}\,dt \tag{A15}$$

for $\lambda \gg 1$ can be obtained in a way similar to that of Watson's Lemma. Note that

$$[1 + e^{\lambda t}]^{-1/2} = e^{-\lambda t/2}[1 + e^{-\lambda t}]^{-1/2} = T(\lambda t) \tag{A16}$$

Let constants K, b, and c exist so that $|f(t)| < K\exp(bt)$ for all $t > c$. Also, f is integrable from (0, c). Clearly $\varphi(\lambda)$ exists for $\lambda > b$. In our case f converges to 1 as t approaches infinity so that $b = 0$. Let us assume that, without loss in generality, $f(t)$ can be written as

$$f(t) = t^{-\beta}(a_0 + a_1t + a_2t^2 + \ldots + a_mt^m + R(t)) \tag{A17}$$

where m is some nonnegative integer and where some constant C exists such that

$$|R(t)| < Ct^{m+1}$$

for t in (0, c). Then

$$\varphi(\lambda) = \int_0^c T(\lambda t)\,t^{-\beta}(a_0 + a_1t + a_2t^2 + \ldots + a_mt^m)\,dt + \int_0^c t^{-\beta}T(\lambda t)\,R(t)\,dt + \int_c^\infty T(\lambda t)\,t^{-\beta}f(t)\,dt \tag{A18}$$

The first integral in eq A18 can be rewritten as

$$\int_0^\infty T(\lambda t)\,t^{-\beta}(a_0 + a_1t + \ldots + a_mt^m)\,dt - \int_c^\infty T(\lambda t)\,t^{-\beta}(a_0 + a_1t + \ldots + a_mt^m)\,dt = \sum_{k=0}^{\infty} a_k(2^{k+1-\beta})\lambda^{-k-1+\beta}I(k-\beta) + O(e^{-\lambda c/2})$$

where the symbol $O(e^{-\lambda c/2})$ means that the last term becomes less in magnitude than some constant times $e^{-\lambda c/2}$ as λ goes to infinity and I is defined by

$$I(-\beta+k) = \int_0^\infty u^{-\beta+k}e^{-u}[1 + e^{-2u}]^{-1/2}\,du$$

The second integral in eq A18 is less than

$$\int_0^\infty t^{-\beta}T(\lambda t)\,Ct^{m+1}\,dt = O(\lambda^{-m-2+\beta})$$

and the third integral in eq A18 is of order $O(e^{(b-\lambda)/2})$ so that it is exponentially small as λ goes to infinity. Altogether, then, we get, as λ goes to infinity

$$\varphi(\lambda) = 2^{1-\beta}\lambda^{-1+\beta}I(-\beta) + \text{higher order terms}$$

The proof for eq 23 follows exactly the same line of reasoning and will not be repeated.

References and Notes

(1) Kramer, E. J. *Adv. Polym. Sci.* **1983**, *52/53*, 1.
(2) Miller, P.; Kramer, E. J. *J. Mater. Sci.* **1991**, *26*, 1459.
(3) Doll, W. *Adv. Polym. Sci.* **1983**, *52/53*.
(4) Wang, W.-C. V.; Kramer, E. J. *J. Mater. Sci.* **1982**, *17*, 2013.
(5) Verhuelpen-Heymans, N. *Polym. Eng. Sci.* **1984**, *24*, 809.
(6) Yang, A.-C. M.; Kramer, E. J.; Kuo, C. C.; Phoenix, S. L. *Macromolecules* **1986**, *19*, 2010.
(7) Yang, A.-C. M.; Kramer, E. J.; Kuo, C. C.; Phoenix, S. L. *Macromolecules* **1986**, *19*, 2020.
(8) Kramer, E. J.; Berger, L. L. *Adv. Polym. Sci.* **1991**, 1.
(9) Brown, H. R. *Macromolecules* **1991**, *24*, 2752.
(10) Miller, P.; Buckley, D. J.; Kramer, E. J. *J. Mater. Sci.* **1991**, *26*, 4445.
(11) Berger, L. L. *Macromolecules* **1989**, *22*, 3162.
(12) Dugdale, D. S. *J. Mech. Phys. Solids* **1960**, *8*, 100.
(13) Barenblatt, G. I. *J. Appl. Math.* **1959**, *23*, 622.
(14) Rice, J. R. Mathematical Analysis in the Mechanics of Fracture. In *Fracture*; Liebowitz, H., Ed.; Academic: New York, 1968; Vol. 2, p 191.
(15) Fager, L. O.; Bassani, J. L.; Hui, C. Y.; Xu, D. B. *Int. J. Fract.*, in press.
(16) Rice, J. R. In *The Mechanics of Quasi-static Crack Growth*, Proceedings of the eighth U.S. National Congress of Applied Mechanics, Kelly R. E., Ed.; 1978; p 191.
(17) Lauterwasser, B. D.; Kramer, E. J. *Philos. Magn.* **1979**, *A39*, 469.
(18) Tada, H.; Paris, P. C.; Irwin, G. R. *The Stress Analysis of Cracks Handbook*; Del Research: St. Louis, MO, 1985.
(19) Creton, C., Kramer, E. J.; Hui, C. Y.; Brown, H. R. Failure Mechanisms of Polymer Interfaces Reinforced with Block Copolymers *Macromolecules*, in press.